https://doi.org/10.5194/egusphere-2023-2751
Preprint. Discussion started: 27 November 2023


# Unveiling Amplified Isolation in Climate Networks due to Global Warming

Yifan Cheng[1], Panjie Qiao[1]*, Meiyi Hou[2], Yuan Chen[1], Wenqi Liu[1] and Yongwen Zhang[1]*

[1.] Data Science Research Center, Faculty of Science, Kunming University of Science and Technology, Kunming 650500, China;

[2.] Department of Atmospheric Sciences, Yunnan University, Kunming, China.

**Correspondence to*: Panjie Qiao(qiaopanjie0720@163.com), and Yongwen Zhang (zhangyongwen77@gmail.com)

**Abstract**

Our study utilizes global reanalysis of near-surface daily air temperature data, spanning from 1949 to 2019, to construct climate networks. By employing community detection for each year, we reveal the evolving community structure of the climate network within the context of global warming. Our findings indicate significant changes in measures such as the network modularity, the number of communities, and the average community size over the past 30 years. Notably, the community structure of the climate network undergoes a discernible transition around 1982. We attribute this transition to the substantial increase in isolated nodes after 1982, primarily concentrated in equatorial ocean regions. Additionally, we demonstrate that nodes experiencing amplified isolation tend to diminish connectivity with other nodes globally, particularly those within the same oceanic basin, while showing a significant strengthening of connections with the Eurasian and North African continents. We propose that the mechanism behind the amplified isolation in the climate network can be understood through weakened

https://doi.org/10.5194/egusphere-2023-2751
Preprint. Discussion started: 27 November 2023


ocean current interactions under global warming.

***Key words*：** *Climate network, community detection, modularity, isolated nodes.*

## 1 Introduction

Since the 20th century, with the continuous increase of greenhouse gas emissions, the global climate system is undergoing warming[1-3]. Climate warming leads to surge in various extreme events, including extreme heat waves, ocean acidification, glaciers melting, drought, floods and hurricanes, etc. [4]. In addition, it has a serious impact on global air quality, food production, energy consumption, transportation, water resources, economic and ecosystems, etc. [5-8]. The elevation in global temperatures has led to substantial alterations in the distribution of heat on Earth, subsequently imparting far-reaching impacts on atmospheric circulation and ocean circulation patterns[9,10]. For example, in the context of global warming, research by Hu et al. (2021) found that the El Niño-Southern Oscillation (ENSO) events with the same amplitude can lead to larger anomalies in the tropospheric water vapor, consequently resulting in more significant global atmospheric circulation, temperature, and precipitation anomalies[11]; Ditlevsen et al. (2023) discovered that with the increasing concentration of greenhouse gases, the Atlantic Meridional Overturning Circulation (AMOC) may collapse around the middle of this century. This will have severe impacts on the climate in the North Atlantic region[12]; Garner et al. (2023) found that due to the warming of the planet and oceans, tropical cyclones in the Atlantic are gradually intensifying, and the number of major hurricanes is also on the rise[13]. This intricate interaction has exacerbated the diversity and uncertainty of the climate phenomenon, and has become a profound challenge facing contemporary society.

The climate system is highly complex, characterized by diversity, multiscale dynamics, and nonlinearity. Unveiling the internal structure of the climate system necessitates the application of sound

https://doi.org/10.5194/egusphere-2023-2751
Preprint. Discussion started: 27 November 2023


research methods. Complex network analysis emerges as a potent tool for investigating the dynamics and structural characteristics of complex systems. Over the past several years, complex network methodologies have gained widespread application in the realm of climate science. By using various climate factors (e.g., precipitation, temperature, wind, etc.), a climate network can be constructed. In the climate network, variables such as temperature or geographical location are used as network nodes, and links are established based on correlations and covariances among climate variables. Through studying the interactions and relationships between nodes, the topological structure of the climate system can be revealed, thereby deepening our comprehension of climate change and climatic phenomena at different spatiotemporal scales. Donges et al. employ linear Pearson correlation coefficients or nonlinear mutual information as measures of dynamic similarity between regions[14].They systematically compare climate networks constructed from the same global climate dataset at local, mesoscale, and global topological scales. Boers et al. used the complex network method to reveal the teleconnection model of global extreme precipitation[15]. Gozolchiani et al. constructed and analyzed a climate network representing interdependent structures of climate across different geographical regions, uncovering its unique response to El Niño events [16]. Methods of climate network analysis have also been employed to identify the weakening of tropical circulation in recent years[17,18] and the correlation between atmospheric activities and pollutants[19]. Furthermore, complex network methods have been utilized to predict El Niño events[20-22]. In summary, complex network analysis is an effective approach for exploring the physical and statistical laws of the Earth's system[23].

A network is a collection of multiple vertices connected by edges[24]. The network's topological structure can unveil important and novel characteristics of the system it represents[25-29]. An important

https://doi.org/10.5194/egusphere-2023-2751
Preprint. Discussion started: 27 November 2023


feature of network is community structure[30]. The community structure is an important feature that reflects the overall structural properties of complex networks. In-depth analysis of the community structure allows for a systematic understanding of the structural relationships and characteristics of complex networks. In a climate network, each community may represent a subsystem. Understanding the community structure can provide a deeper insight into the interrelationships between different components of the climate system. Communities can be associated with network functionality, as seen in the identification of genomic sets responsible for specific functions in metabolic networks[31].Currently, there are many researches on the internal dynamics mechanism of climate system based on community structure. For example, Tsonis et al. (2011)[32] constructed climate networks using observed climate variables and model simulations, and investigated their community structure. Agarwal et al. (2018)[33] identified communities using community detection algorithms to quantify the influence of individual rainfall stations within homogeneous regions. Some studies have identified novel dynamic mechanisms of climate systems through the characteristics of community structures in networks [34-37]. However, few studies have considered the effects of global warming on the community structure of climate networks. Therefore, the research aims to use network analysis and community detection to explore how global warming is altering the structure of the global temperature network, with the ultimate goal of advancing our understanding of climate change and informing strategies to address its impacts.

Therefore, based on the near-surface temperature structure climate network, this paper studies the impact of global warming on climate network. Employing the Louvain community detection algorithm, it analyzes the evolution of network topology and reveals the underlying factors driving changes in the network structure. The main structure of this paper is as follows: Section 2 introduces the data and

https://doi.org/10.5194/egusphere-2023-2751
Preprint. Discussion started: 27 November 2023


methods; Section 3 discusses the evolution of climate network topology in the context of global warming; Section 4 summarizes the results.

## 2 Data

This study utilizes daily air temperature reanalysis data from the National Centers for Environmental Prediction (NCEP) and the National Center for Atmospheric Research (NCAR) at a resolution of $2.5° \times 2.5°$, spanning the near-surface (sig995 level) temperatures from 1949 to 2019. The dataset comprises 10,512 grid points over the global. For simplification purposes, we strategically select 726 nodes (grid points) to construct the network and ensure uniform global coverage with same distance interval.

## 3 Methods

### 3.1 Constructing the climate network

Climate networks are constructed based on the near-surface air temperature data for each year from 1949 to 2019, resulting in a total of 71 established climate networks. The time series of a node (denoted as $i$) is detrended by subtracting the average seasonal cycle and dividing by the standard deviation of the cycle to obtain the temperature anomaly (denoted as $T_i^y(t)$, where $y$ is the index of year) [19]. To obtain the link strength between each pair of nodes $i$ and $j$, we then calculate the time-lagged cross-correlation function[38]:

$$C_{i,j}^{y}(-\tau) = \frac{\langle T_i^y(t) T_j^y(t-\tau)\rangle - \langle T_i^y(t)\rangle \langle T_j^y(t-\tau)\rangle}{\sqrt{\langle (T_i^y(t) - \langle T_i^y(t)\rangle)^2\rangle} \cdot \sqrt{\langle (T_j^y(t-\tau) - \langle T_j^y(t-\tau)\rangle)^2\rangle}}, \quad (1)$$

$$C_{i,j}^{y}(\tau) = \frac{\langle T_i^y(t-\tau) T_j^y(t)\rangle - \langle T_i^y(t-\tau)\rangle \langle T_j^y(t)\rangle}{\sqrt{\langle (T_i^y(t-\tau) - \langle T_i^y(t-\tau)\rangle)^2\rangle} \cdot \sqrt{\langle (T_j^y(t) - \langle T_j^y(t)\rangle)^2\rangle}}, \quad (2)$$

https://doi.org/10.5194/egusphere-2023-2751
Preprint. Discussion started: 27 November 2023


where ⟨ ⟩ denotes the mean value, based on which $\langle f(a)\rangle = \frac{1}{365}\sum_{t=1}^{365} f(t-a)$; $t$ represents time and the time lag is denoted as $\tau \in [0,200]$.

Therefore, the link strength between each pair of nodes in the network is denoted as follows:

$$W_{i,j}^{y} = \frac{max(C_{i,j}^{y}) - mean(C_{i,j}^{y})}{std(C_{i,j}^{y})}, \quad (3)$$

in this context, “$max$”,”$mean$” and “$std$” refer to the maximum value, minimum value, mean, and standard deviation of the cross-correlation functions. The cross-correlation can be inflated due to the autocorrelation of points. The strength $W_{i,j}^{y}$ reflects the deviation and serves to eliminate the effect of autocorrelation, aiming for a more desirable outcome. To select meaningful links in the network and eliminate false associations, we retain the top 5% of links in the network such that a threshold of $\theta = 3.5$ is applied to obtain an adjacency matrix $A$ (when $W_{i,j}^{y} \geq \theta$, the element $A_{ij} = 1$, otherwise, the element $A_{ij} = 0$).

### 3.2 Community Detection

Subsequently, the obtained sequence of climate networks underwent community detection using the Louvain community detection algorithm. The key steps of this method involve traversing each node in the network and attempting to relocate it to a neighboring node in a different community to optimize the modularity $Q$. If moving a node to another community increases the modularity, the move is executed; otherwise, it remains unchanged. In other words, the process assesses whether the increment in modularity $\Delta Q$ resulting from the move is positive, and this procedure is repeated until no further node movements are possible. Here is the formula for calculating modularity[27]:

$$Q = \frac{1}{2m}\sum_{i,j}\left[A_{ij} - \frac{k_i k_j}{2m}\right]\delta(c_i, c_j), \quad (4)$$

Where $k_i = \sum_j A_{ij}$ and $k_j = \sum_i A_{ij}$ are the sums of the weights of links connected to vertex $i$ and vertex $j$ (i.e., the number of links connected to node $i$ and node $j$), $c_i$ represents the community to which node $i$ belongs, $\delta(\mu, v)$ equals 1 if $\mu = v$, otherwise 0, and $m = \frac{1}{2}\sum_{ij} A_{ij}$. Modularity has become a metric for assessing the quality of community divisions, with high modularity indicating strong internal connections within a community and weaker connections with other communities.

https://doi.org/10.5194/egusphere-2023-2751
Preprint. Discussion started: 27 November 2023


## 4 Results

In order to investigate the evolution of the network's topology in the context of global warming, we construct the network for each year from 1949 to 2019 and apply community detection to the network. In Figure 1(a), we show that the network modularity for the early years (1949-1981) is largely below the average level. While in the recent years (1982-2019), the network modularity remain consistently above the average level. There is a significant transition in the modularity around 1982. The number of communities and modularity exhibit similar evolutionary patterns as shown in Figure 1(b). Although the trend in the change of the number of communities is not as pronounced as the trend in network modularity, it is still evident that the number of communities was mostly below the average level in the first 33 years, while in the recent 38 years, the majority of community numbers are above the average level (as shown in Figure 1(b)). The trend in the average community size exhibits the opposite pattern compared to modularity and the number of communities, but similarly experiences a noticeable transition around 1982. Figure 1(c) shows that before 1982, the average community size is mostly above the average level, while after 1982, the average community size is mostly below the average level. The evolution of network modularity, the number of communities, and the average community size all underwent a transition around 1982. A very strong El Niño event occurred between 1982 and 1983. The event have a profound impact on the global climate and caused the global seawater temperature to increase [39].

https://doi.org/10.5194/egusphere-2023-2751
Preprint. Discussion started: 27 November 2023


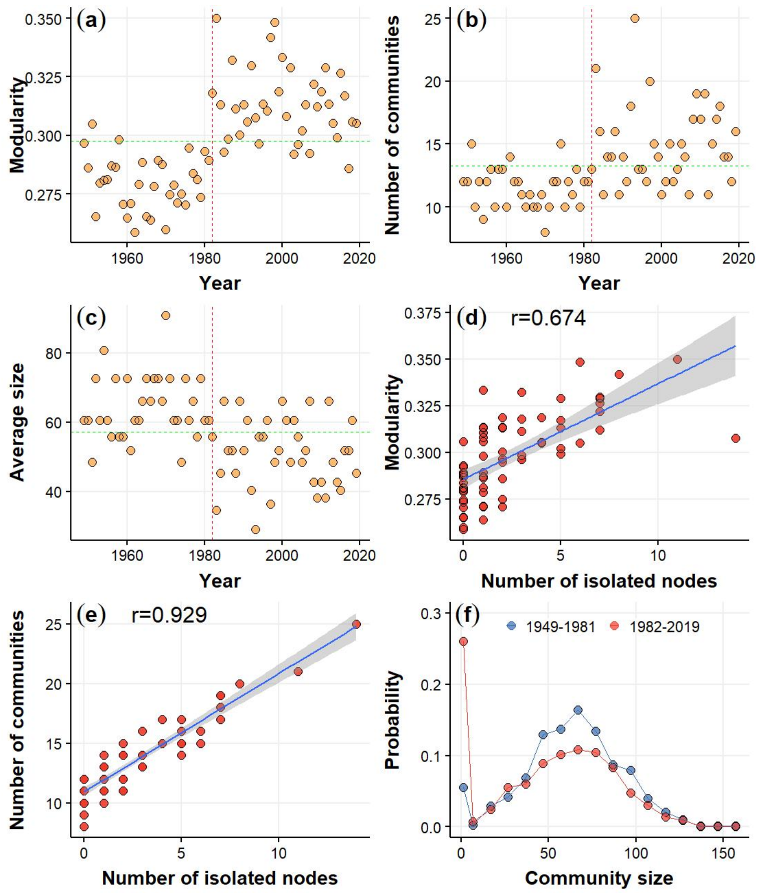


**Figure 1: Temporal evolution of (a) network modularity, (b) the number of communities and (c) the average size of communities from 1949 to 2019, illustrated by the green dashed line denoting the average level, and the red dashed line represents the transition around 1982. Scatter plot of (d) the network modularity, (e) the number of communities versus the number of isolated nodes during the period 1949-2019. (f) The probability distribution of community size for 1949-1981 and 1982-2019 respectively, where the starting dot represents the probability of the isolated node.**

After 1982, the number of communities increases, while their average size decreases. We find that this is related to the number of isolated nodes (with the community size 1). We observe the relationship between modularity and the number of isolated nodes and find a strong positive correlation with a correlation coefficient of 0.674 (as shown in Figure 1(d)). The high correlation with network

https://doi.org/10.5194/egusphere-2023-2751
Preprint. Discussion started: 27 November 2023


modularity indicates that the trend in the number of isolated nodes is consistent with changes in the network's topological structure. Furthermore, from Figure 1(e), we observe that the correlation between the number of isolated nodes and the number of communities reaches 0.929. The high correlation with the number of communities suggests that the overall increase in the number of communities is driven by the increase in isolated nodes. To further strengthen the verification of whether the changes in the number of communities, network modularity, and average community size after 1982 are related to the number of isolated nodes. We examine the probability distribution of community sizes in 1949-1981 and 1982-2019 (as shown in Figure 1(f)). There are two peaks for the isolated node and the community with size around 60 in the probability distribution of community size for both 1949-1981 and 1982-2019. In 1949-1981, the proportion of isolated nodes in the overall community is not prominent. However, in 1982-2019, the proportion of isolated nodes has dramatically increased and has become the largest component in the community distribution. Therefore, the transition in modularity, the number of communities, and average community size in 1982 can be attributed to the substantial increase in the number of isolated nodes.

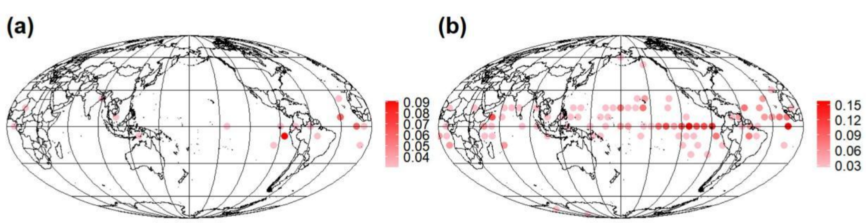


**Figure 2: Occurrence probability maps of isolated nodes for (a) 1949-1981, and (b) 1982-2019.**

Next, we will further study the relationship between changes in climate network structure and isolated nodes. The occurrence probability maps of isolated nodes for 1949-1981 and 1982-2019 are

https://doi.org/10.5194/egusphere-2023-2751
Preprint. Discussion started: 27 November 2023


shown in Figure 2. From 1949 to 1981, few isolated nodes are mainly distributed in the Equatorial East Pacific and Equatorial Atlantic oceans, with a low occurrence probability. However, from 1982 to 2019, the isolated nodes with higher occurrence probabilities can appear almost everywhere in the equatorial regions such that the total number of communities increase. The occurrence probability of isolated nodes in the last 38 years is not only higher than the first 33 years but also covers a larger area than the first 33 years. As global warming progresses, the isolated nodes in the equatorial region are increasing, leading to changes in the climate network structure where the nodes are less connected to each other, resulting in more independent communities with smaller community sizes.

To gain a deeper understanding and verify how the isolation in climate networks is amplified in the Equatorial regions, we select three nodes with the highest frequency of isolation in three regions: the Indian Ocean, the Pacific Ocean, and the Atlantic Ocean, respectively. We study the relationships between the three nodes and other nodes across the climate network structure. Specifically, we calculate the probability of the selected node and each of other 725 nodes belonging to the same community for time periods 1949-1981 and 1982-2019, and compute the difference the two time periods. This probability can reflect which important region responds to the amplified isolation of the selected node.

In Figure 3(a), for 1949-1981, the selected Indian Ocean node exhibits high probability with surrounding nodes belonging to the same community. However, for the 1982-2019 in Figure 3(b), this probability is weakened, particularly in their association with the oceanic regions. the difference of the probability between 1982-2019 and 1949-1981 is shown in Figure 3(c). Blue (red) points in Figure 3(c) represent the decreased (increased) probability with time. In general, most areas have decreased probability. Still, some areas i.e., the Eurasian and North Africa continent have increased probability to

https://doi.org/10.5194/egusphere-2023-2751
Preprint. Discussion started: 27 November 2023


connect to the selected Indian Ocean node.

With global warming, the probabilities of the nodes in the Pacific and the equatorial Pacific region belonging to the same community are noticeably diminished (as shown in Figure 4). Examining the probability map of the selected Atlantic Ocean node and other global nodes belonging to the same community in Figure 5, it is observed a similar behavior. The selected three high-frequency isolated nodes are surrounded by relatively strong connectivity regions during the first 33 years. However, these regions experience varying degrees of weakening in connectivity during the subsequent 38 years. It is worth noting that with global warming, the connectivity between high-frequency isolated nodes in the Indian Ocean, Atlantic Ocean, and Pacific Ocean with global oceanic regions is diminishing, especially the strength of their connections with their respective oceanic regions significantly decreasing. However, the association with the Eurasian and North Africa continent is strengthening. The research indicates that widespread changes in surface temperature persistence under climate change, this change is usually robust in the ocean. Averaged model results suggest a weakening of persistence in tropical regions[40]. Moreover, as global warming advances, ocean stratification intensifies, the mixed layer depth diminishes, and ocean memory and oceanic persistence weakens[41]. As global warming continues to reshape ocean temperatures and melt ice sheets, the influx of melted ice introduces a substantial volume of freshwater into the ocean. This infusion of freshwater diminishes ocean salinity gradients, consequently weakening ocean currents[42-44]. Therefore, there are fewer nodes associated with tropical oceans and their internal dynamics, while isolated nodes increase. Furthermore, climate change also modifies large-scale circulation patterns, and intensifies ocean-atmosphere interactions, land-atmosphere interactions, thereby strengthening the linkage between equatorial regions and the continent.

https://doi.org/10.5194/egusphere-2023-2751
Preprint. Discussion started: 27 November 2023


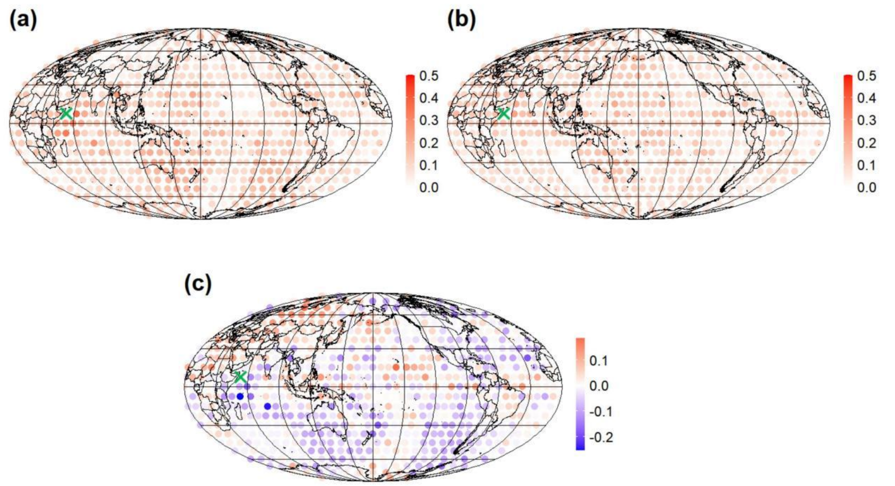


**Figure 3: Probability maps of the Indian Ocean node and other global nodes belonging to the same community for (a) 1949-1981, (b) 1982-2019, and (c) the difference of the probability between 1982-2019 and 1949-1981. The symbol of cyan cross represents the selected Indian Ocean node.**

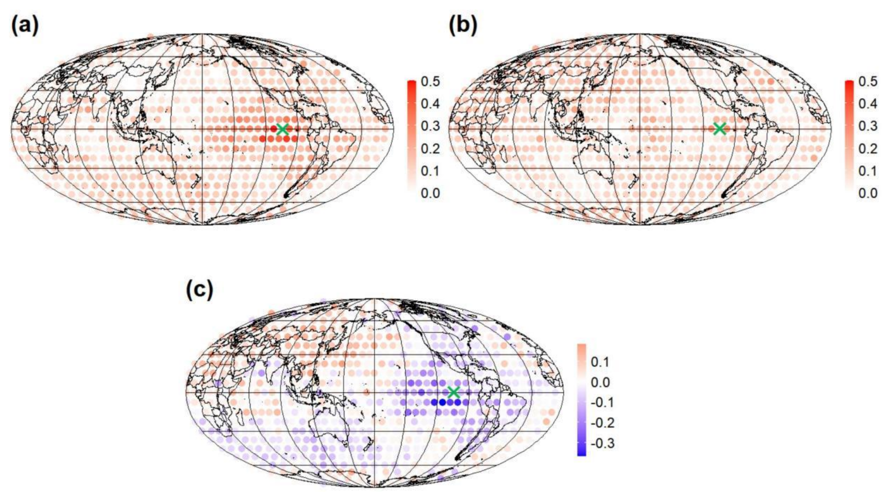

https://doi.org/10.5194/egusphere-2023-2751
Preprint. Discussion started: 27 November 2023


**Figure 4: Probability maps of the Eastern Pacific Ocean node and other global nodes belonging to the same community for (a) 1949-1981, (b) 1982-2019, and (c) the difference of the probability between 1982-2019 and 1949-1981. The symbol of cyan cross represents the selected Eastern Pacific Ocean node.**

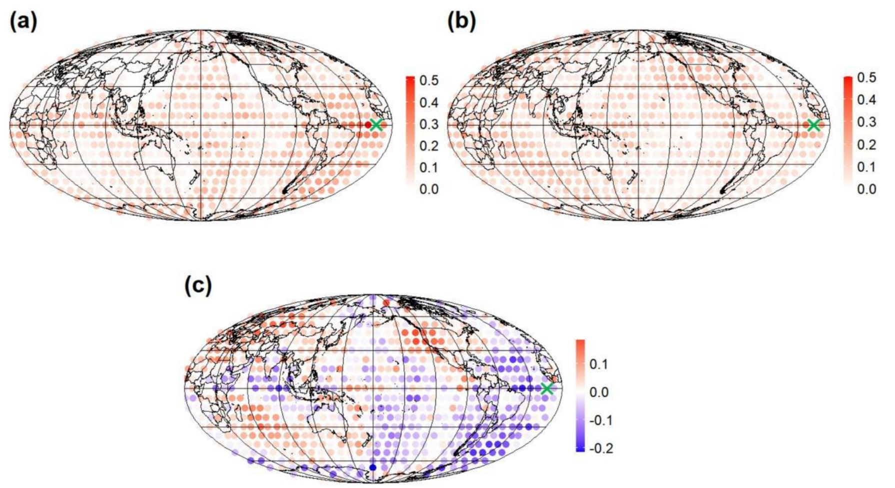


**Figure 5: Probability maps of the Atlantic Ocean node and other global nodes belonging to the same community for (a) 1949-1981, (b) 1982-2019, and (c) the difference of the probability between 1982-2019 and 1949-1981. The symbol of cyan cross represents the selected Atlantic Ocean node.**

## 5 Conclusions

In this investigation, we constructed a climate network using near-surface air temperature data spanning from 1949 to 2019. Our aim was to examine the evolution of climate network topology within the context of global warming. To explore how global warming affects the structure of the global climate network, we applied the Louvain community detection algorithm. Our overarching goal was to

https://doi.org/10.5194/egusphere-2023-2751
Preprint. Discussion started: 27 November 2023


enhance our comprehension of climate change and contribute to the formulation of strategies to mitigate its impacts.

Notably, we observed that the network modularity between 1949 and 1981 remained below the overall average, whereas between 1982 and 2019, it exceeded the overall average. Concurrently, the trend in the number of communities from 1949 to 2019 followed a similar pattern to that of modularity. Conversely, the trend in average community size exhibited an opposite pattern to that of modularity and community quantity. Specifically, the average community size consistently exceeded the average during the initial 33 years but predominantly fell below the average in the subsequent 38 years. Furthermore, the correlation coefficient between modularity and the number of isolated nodes was found to be 0.674. Additionally, the correlation between the number of isolated nodes and the number of communities reached 0.929, both of which demonstrated statistical significance. Furthermore, we noted a substantial increase in the number of isolated nodes after 1982. Hence, the shift in modularity, the number of communities, and average community size in 1982 are significantly associated with the notable surge in the number of isolated nodes.

As global warming continues, the prevalence of isolated nodes is on the rise. Between 1949 and 1981, isolated nodes were sporadic and dispersed, mainly concentrated in the equatorial Pacific and equatorial Atlantic regions. However, from 1982 to 2019, isolated nodes were pervasive across the entire equatorial oceanic region. We further examined the relationship between temperature network structure and isolated nodes in the context of global warming. By selecting key nodes with the highest frequency of isolation in the equatorial Pacific, equatorial Atlantic, and equatorial Indian Ocean regions, we investigated their likelihood of belonging to the same community as other nodes during 1949-1981 and 1982-2019. Our findings indicate that, amidst global warming, the connectivity of highly isolated nodes along the equator is diminishing, particularly concerning their associations with neighboring regions within the same oceanic basin, while their connections with certain continents have significantly strengthened.

**Data Availability**

The data that supports the findings of this study are publicly available online: NCEP/NCAR reanalysis near-surface (sig995 level) daily air temperature data, https://www.esrl.noaa.gov/psd/data/gridded/data.ncep.reanalysis. derived.surface.html, accessed on 14 September 2022.

**Author Contributions**

**CYF, QPJ, HMY, CY, LWQ and ZYW:** Conceptualization, Investigation, Methodology, Visualization, Writing, Review. **CYF, QPJ, HMY, CY, LWQ and ZYW:** Conceptualization, Investigation, Methodology, Writing, Review. **CYF, QPJ, HMY, CY, LWQ and ZYW:** Conceptualization, Writing, Review. **CYF, QPJ, HMY, CY, LWQ and ZYW:** Methodology, Supervision, Funding Acquisition, Writing. **CYF, QPJ, HMY, CY, LWQ and ZYW:** Conceptualization, Investigation, Methodology, Writing, Review, Funding Acquisition.

**Competing interests**

The contact author has declared that none of the authors has any competing interests.

**Disclaimer**

Publisher's note: Copernicus Publications remains neutral with regard to jurisdictional claims in published maps and institutional affiliations.

**Acknowledgements**

This study was supported by the National Natural Science Foundation of China (No. 12305044 and No. 12371460) and the Fundamental Research Program of Yunnan Province (No. CB22052C173A).

**References**

[1] B. F. Christopher, V. Barros, T. F. Stocker and Q. Dahe: Managing the Risks of Extreme Events and Disasters to Advance Climate Change Adaptation: Special Report of the Intergovernmental Panel on Climate Change, Cambridge University Press: Cambridge, UK (2012). https://doi.org/10.1017/CBO9781139177245

[2] S. Hallegatte, V. Przyluski and A. Vogt-Schilb: Building world narratives for climate change impact, adaptation and vulnerability analyses, Nat. Clim. Change 1, 151–155 (2011). https://doi.org/10.1038/ nclimate1135

[3] A. Hunt and P. Watkiss: Climate change impacts and adaptation in cities: a review of the literature, Clim. Change 104, 13–49 (2011). https://doi.org/10.1007/s10584-010-9975-6

[4] Scott C Doney , Victoria J Fabry, Richard A Feely and Joan A Kleypas: Ocean Acidification: The Other CO2 Problem, Annu. Rev. Mar. Sci. 1, 169-192 (2009). https://doi.org/10.1146/annurev.marine.010908.163834

[5] Chris D. Thomas, Alison Cameron, Rhys E. Green, Michel Bakkenes, Linda J. Beaumont, Yvonne C. Collingham, Barend F. N. Erasmus, Marinez Ferreira de Siqueira, Alan Grainger, Lee Hannah, Lesley Hughes, Brian Huntley, Albert S. van Jaarsveld, Guy F. Midgley, Lera Miles, Miguel A. Ortega-Huerta, A. Townsend Peterson, Oliver L. Phillips and Stephen E. Williams: Extinction risk from climate change, Nature 427, 145–148 (2004). https://doi.org/10.1038/nature02121

[6] I. Salehyan and C.S. Hendrix: Climate shocks and political violence, Glob. Environ. Change 28, 134-145 (2014). https://doi.org/10.1016/j.gloenvcha.2014.07.007

[7] Nordhaus and William D.: Revisiting the social cost of carbon, Proc Natl Acad Sci USA 114(7), 1518 (2017). https://doi.org/10.1073/pnas.1609244114

[8] M. Burke, S. Hsiang, E. and Miguel: Global non-linear effect of temperature on economic production, Nature 527, 235–239 (2015). https://doi.org/10.1038/nature15725

[9] R. Sutton and B. Dong: Atlantic Ocean influence on a shift in European climate in the 1990s, Nat. Geosci. 5, 788–792 (2012). https://doi.org/10.1038/ngeo1595

[10] T. Schneider, T. Bischoff and G. Haug: Migrations and dynamics of the intertropical convergence zone, Nature 513, 45–53 (2014). https://doi.org/10.1038/nature13636

[11] K. Hu, G. Huang and P. Huang: Intensification of El Niño-induced atmospheric anomalies under greenhouse warming, Nat. Geosci. 14, 377–382 (2021). https://doi.org/10.1038/s41561-021-00730-3

[12] P. Ditlevsen and S. Ditlevsen: Warning of a forthcoming collapse of the Atlantic meridional overturning circulation, Nat. Commun. 14, 4254 (2023). https://doi.org/10.1038/s41467-023-39810-w

[13] A.J. Garner: Observed increases in North Atlantic tropical cyclone peak intensification rates, Sci. Rep. 13, 16299 (2023). https://doi.org/10.1038/s41598-023-42669-y

[14] J. F. Donges, Y. Zou, N. Marwan and J. Kurths: Complex networks in climate dynamics, Eur. Phys. J. Spec. Top. 174, 157–179 (2009). https://doi.org/10.1140/epjst/e2009-01098-2

[15] Niklas Boers, Bedartha Goswami, Aljoscha Rheinwalt, Bodo Bookhagen, Brian Hoskins and Jürgen Kurthsl: Complex networks reveal global pattern of extreme-rainfall teleconnections, Nature 566, 373–377 (2019). https://doi.org/10.1038/s41586-018-0872-x

[16] A. Gozolchiani, S. Havlin and K. Yamasaki: Emergence of El Niño as an autonomous component in the climate network, Phys. Rev. Lett. 107(14), 148501 (2011). https://doi.org/10.1103/PhysRevLett.107.148501

[17] Y. Zhang, J. Fan, X. Chen, Y. Ashkenazy and S. Havlin: Significant Impact of Rossby Waves on Air Pollution Detected by Network Analysis, Geophys. Res. Lett. (2019). https://doi.org/10.1029/2019GL084649

[18] Z. Geng, Y. Zhang, B. Lu, J. Fan, Z. Zhao and X. Chen: Network-Synchronization Analysis Reveals the Weakening Tropical Circulations, Geophys. Res. Lett. 48, e2021GL093582 (2021). https://doi.org/10.1029/2021GL093582

[19] J. Fan, J. Meng, Y. Ashkenazy, S. Havlin and H. J. Schellnhuber: Climate Network Percolation Reveals the Expansion and Weakening of the Tropical Component Under Global Warming, Proc. Natl. Acad. Sci. U.S.A. 115(49), E12128–E12134 (2018). https://doi.org/10.1073/pnas.1811068115

[20] J. Ludescher, A. Gozolchiani, M. I. Bogachev, A. Bunde, S. Havlin and H. J. Schellnhuber: Very Early Warning of Next El Niño, Proc. Natl. Acad. Sci. U.S.A. 111, 2064–2066 (2014). https://doi.org/10.1073/pnas.1323058111

[21] J. Fan, J. Meng, Y. Ashkenazy, S. Havlin and H. J. Schellnhuber: Network Analysis Reveals Strongly Localized Impacts of El Niño, Proc. Natl. Acad. Sci. U.S.A. 114, 7543–7548 (2017).

https://doi.org/10.1073/pnas.1701214114

[22] J Meng, J. Fan, Y. Ashkenazy, A. Bunde and S. Havlin: Forecasting the Magnitude and Onset of El Niño Based on Climate Network, New J. Phys. 20, 043036 (2018). https://doi.org/10.1088/1367-2630/aabb25

[23] J. Fan, J. Meng, J. Ludescher, X. Chen, Y. Ashkenazy, J. Kurths, S. Havlin and H. J. Schellnhuber: Statistical Physics Approaches to the Complex Earth System, Phys. Rep. 896, 1–84 (2020). https://doi.org/10.1016/j.physrep.2020.09.005

[24] R. Albert and A. L. Barabasi: Statistical Mechanics of Complex Networks, Rev. Mod. Phys. 74, 1–54 (2002). https://doi.org/10.1103/RevModPhys.74.47

[25] S. Strogatz: Exploring complex networks, Nature 410, 268–276 (2001). https://doi.org/10.1038/35065725

[26] L. da F. Costa , F. A. Rodrigues , G. Travieso and P. R. Villas Boas: Characterization of complex networks: a survey of measurements, Adv. Phys. 56, 167–242 (2007). https://doi.org/10.1080/00018730601170527

[27] V. D. Blondel, J. L. Guillaume, R. Lambiotte and E. Lefebvre: Fast unfolding of communities in large networks, J. Stat. Mech. 10(10), P10008 (2008). https://doi.org/10.1088/1742-5468/2008/10/P10008

[28] P. Holme, M. Huss and H. Jeong: Modularity and the spread of perturbations in complex dynamical systems, Chaos 13(3), 913-924 (2003). https://doi.org/10.1103/PhysRevE.92.060801

[29] P. Holme, M. Huss and H. Jeong: Subnetwork hierarchies of biochemical pathways, Bioinformatics 19, 532–538 (2003). https://doi.org/10.1093/bioinformatics/btg033

[30] R Guimerà and L. Nunes Amaral: Functional cartography of complex metabolic networks, Nature 433, 895–900 (2005). https://doi.org/10.1038/nature03288

[31] K. Li, M. Wang and K. Liu: The study of temperature regionalization in China using complex networks, Int. J. Climatol. 42(8), 4445-4459 (2021). https://doi.org/10.1002/joc.7478

[32] Anastasios A. Tsonis, Geli Wang, Kyle L. Swanson, Francisco A. Rodrigues and Luciano da Fontura Costa: Community structure and dynamics in climate networks, Clim. Dyn. 37, 933–940 (2011). https://doi.org/10.1007/s00382-010-0874-3

[33] A. Agarwal, N. Marwan and R. Maheswaran: Quantifying the Roles of Single Stations Within Homogeneous Regions Using Complex Network Analysis, J. Hydrol. 563, S0022169418304724-

https://doi.org/10.5194/egusphere-2023-2751
Preprint. Discussion started: 27 November 2023


(2018). https://doi.org/10.1016/j.jhydrol.2018.06.050

[34] A. A. Tsonis, K. L. Swanson and S. Kravtsov: A new dynamical mechanism for major climate shifts, Chaos 17(3), 033119 (2007). https://doi.org/10.1029/2007GL030288

[35] A. Gozolchiani, K. Yamasaki, O. Gazit and S. Havlin: Pattern of climate network blinking links follow El Niño events, Chaos 18(4), 043107 (2008). http://dx.doi.org/10.1209/0295-5075/83/28005

[36] K. L. Swanson and A. A. Tsonis: Has the climate recently shifted? Geophys. Res. Lett. 36(6) (2009). https://doi.org/10.1029/2008GL037022

[37] J. B. Elsner, T. H. Jagger and E. A. Fogarty: Visibility network of United States hurricanes, Geophys. Res. Lett. 36(16) (2009). https://doi.org/10.1029/2009GL039129

[38]Jingfang Fan , Jun Meng, Josef Ludescher, Zhaoyuan Li, Elena Surovyatkina, Xiaosong Chen, Jürgen Kurths, and Hans Joachim Schellnhuber: Network-based Approach and Climate Change Benefits for Forecasting the Amount of Indian Monsoon Rainfall, Am. Meteorol. Soc.35(3), 1009 – 1020 (2021). https://doi.org/10.1175/JCLI-D-21-0063.1

[39] D.V. Hansen: Physical Aspects of the El Niño Event of 1982–1983, Elsevier Oceanography Series 52, 1-20 (1990). https://doi.org/10.1016/S0422-9894(08)70031-X

[40] J. Li and D. W. J. Thompson: Widespread changes in surface temperature persistence under climate change, Nature 599, 425-430 (2021). https://doi.org/10.1038/s41586-021-03943-z

[41] Hui Shi, Fei-Fei Jin, Robert C. J. Wills, Michael G. Jacox, Dillon J. Amaya, Bryan A. Black, Ryan R. Rykaczewski, Steven J. Bograd, Marisol Garcia-Reyes and William J. Sydeman: Global decline in ocean memory over the 21st century, Sci. Adv. 8, eabm3468 (2022). https://doi.org/10.1126/sciadv.abm3468

[42] D. A. Smeed, S. A. Josey, C. Beaulieu, W. E. Johns, B. I. Moat, E. Frajka-Williams, D. Rayner, C. S. Meinen, M. O. Baringer, H. L. Bryden and G. D. McCarthy: The North Atlantic Ocean Is in a State of Reduced Overturning, Geophys. Res. Lett. 45(3) (2018). https://doi.org/10.1002/2017GL076350

[43] Stefan Rahmstorf, Jason E. Box, Georg Feulner, Michael E. Mann, Alexander Robinson, Scott Rutherford and Erik J. Schaffernicht: Exceptional twentieth-century slowdown in Atlantic Ocean overturning circulation, Nat. Clim. Change 5, 475–480 (2015). https://doi.org/10.1002/2017GL076350

[44] P. J. Webster, G. J. Holland, J.A. Curry and H. R. Chang: Changes in tropical cyclone number, duration, and intensity in a warming environment, Science 309(5742), 1844-1846 (2005). http://dx.doi.org/10.1126/science.1116448